Electronic Supplementary Material

MnO_2 nanosheets@nitrogen-doped graphene aerogel enable high specific energy and high specific power for supercapacitor and Zn-air battery

*Hui Zhao[a], Rijuan Jiang[a], Yong Zhang[a], Beibei Xie[a], Jiali Fu[a], Xiaona Yuan[a], Wenxin Yang[a], Yan Wu[a], and Renjie Zhang[a,b,c]**

[a] Key Laboratory of Colloid and Interface Chemistry of the Ministry of Education of the P. R. China, Shandong University, Jinan 250100, P. R. China

[b] Key Laboratory of Special Functional Aggregated Materials of the Ministry of Education of the P.R. China, Shandong University, Jinan 250100, P. R. China

[c] National Engineering Technology Research Center for Colloidal Materials, Shandong University, Jinan 250100, P. R. China

*Corresponding author, Email: zhrj@sdu.edu.cn

EXPERIMENTAL

Synthesis of GO

GO was prepared by modified Hummers' method,[1] followed by washing several times with 5% HCl and water. Then GO was sonicated (300 W) for 8 h below 25 ^{o}C.[2] Finally, a homogeneous GO aqueous suspension was obtained and used for preparation of NGA and MNSs@NGA.

Calculation of the ratio of exposed surficial unit cells

The ratio of exposed surficial unit cells is calculated by dividing number of exposed surficial unit cells (N_1) by total number of unit cells (N_2) according to the following equation (S1):

$$\text{Ratio of exposed unit cells} = \frac{N_1}{N_2} = \frac{S_1/S_2}{V_1/V_2} \quad \text{(S1)}$$

Where S_1 is surface area of three exposed surface of a single MnO_2 nanosheet, S_2 is area of the rhombus section of a [MnO_6] regular octahedron, V_1 is volume of a single MnO_2 nanosheet and V_2 is volume of a [MnO6] regular octahedron. Assuming the MnO_2 nanosheet is a cuboid, the length, width and height of the cuboid are 100, 50 and 5 nm, respectively. V_1 is 25000 nm^3 and S_1 is 10000 nm^2. V_2 is 0.086 nm^3 and S_2 is 0.092 nm^2. Therefore, the ratio of exposed surficial unit cells is 37.4%.

SUPPLEMENTARY FIGURES AND TABLES

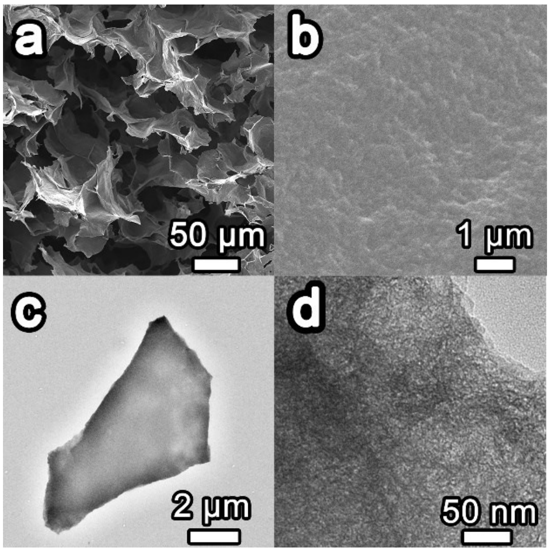

Fig. S1 (a, b) SEM images and (c, d) TEM images of NGA at different magnifications.

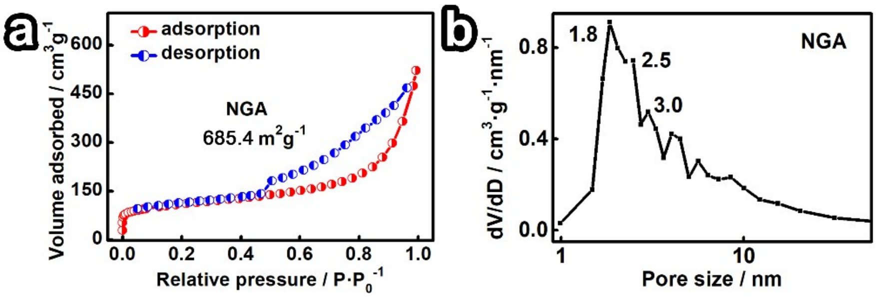

Fig. S2 (a) N_2 adsorption-desorption isotherms at -196 ^oC and (b) pore size distribution of NGA.

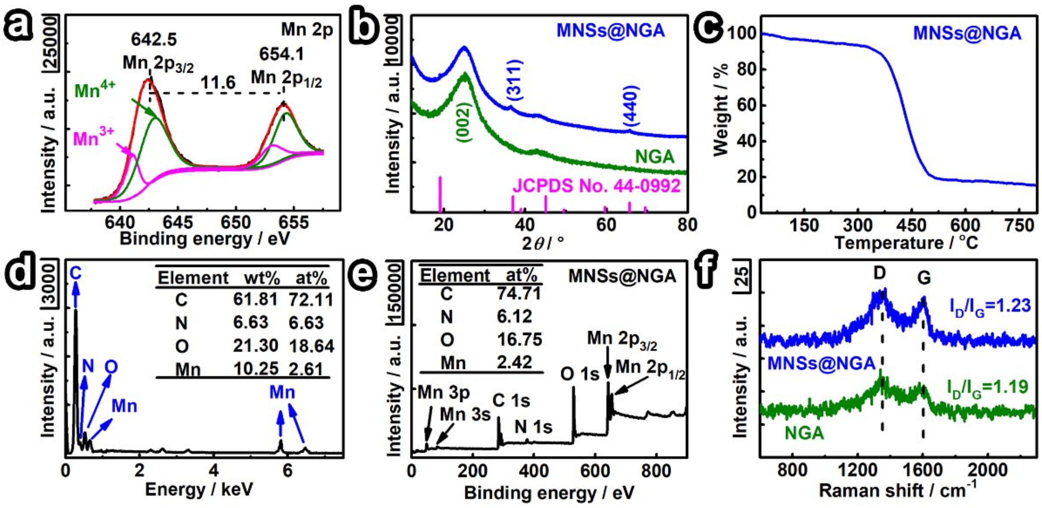

Fig. S3 (a) Mn 2p XPS spectrum of MNSs@NGA. (b) XRD patterns of MNSs@NGA, NGA and λ-MnO_2 (JCPDS 44-0992). (c) TGA curve of MNSs@NGA. (d) EDX spectrum and quantitative analysis of MNSs@NGA. (e) Sum XPS spectrum and quantitative analysis of MNSs@NGA. (f) Raman spectra of MNSs@NGA and NGA.

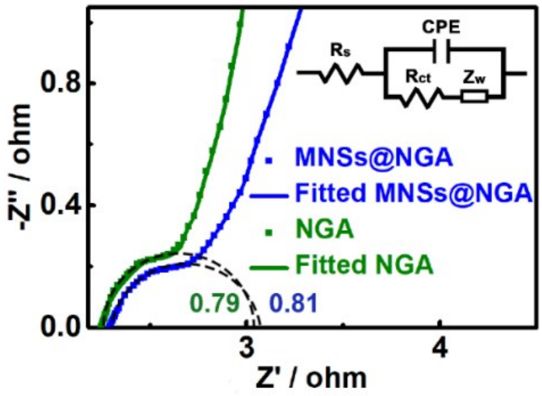

Fig. S4 Nyquist plots of MNSs@NGA and NGA from EIS measurements in O_2-saturated 0.1 M KOH solution.

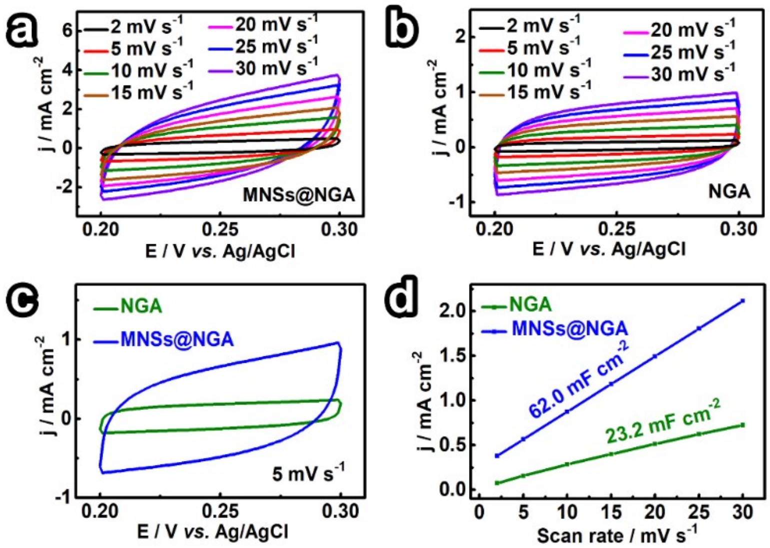

Fig. S5 CV curves of (a) MNSs@NGA and (b) NGA at different scan rates in 1.0 M KOH at the voltage range of 0.20-0.30 V (*vs.* Ag/AgCl). (c) CV curves at a scan rate of 5 mV s^{-1} and (d) the current density at 0.25 V (*vs.* Ag/AgCl) against scan rate of MNSs@NGA and NGA.

Table S1 Comparison of supercapacitor performance between MNSs@NGA and reported MnO_x-based materials

Sample	Morphology	Specific surface area / $m^2 g^{-1}$	Voltage window / V	Electrolyte	Specific capacitance / $F g^{-1}$	Rate capability	Cycling stability	Ref.
CNT/MnO_2/rGO	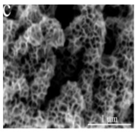	--	0-0.8	1.0 M Na_2SO_4	298 at 0.5 A g^{-1}	207.0 F g^{-1} at 10 A g^{-1}	90.3% after 5000 cycles at 10 A g^{-1}	Carbon 2018, 132, 776.
MnO_2/GO composites	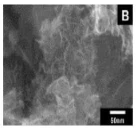	162.0	0.1-0.9	1.0 M Na_2SO_4	297 at 5 mV s^{-1}	268.0 F g^{-1} at 50 mV s^{-1}	--	Small 2015, 11 (11), 1310-1319.
bowl-like MnO_2 nanosheets	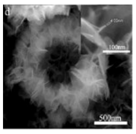	182.4	0-0.8	1.0 M Na_2SO_4	379 at 0.5 A g^{-1}	229.0 F g^{-1} at 10 A g^{-1}	87.3% after 5000 cycles at 0.5 A g^{-1}	Chem. Eng. J. 2018, 350, 79.
diatom/MnO_2	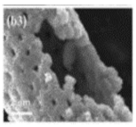	67.3	-0.2-0.8	1.0 M Na_2SO_4	371.2 at 0.5 A g^{-1}	203.0 F g^{-1} at 10 A g^{-1}	93.1% after 2000 cycles at 5 A g^{-1}	J. Mater. Chem. A 2015, 3 (15), 7855-7861.
MnO_2-NHCSs	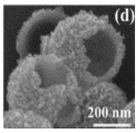	213.1	-0.1-0.9	1.0 M Na_2SO_4	392 at 0.5 A g^{-1}	222.0 F g^{-1} at 10 A g^{-1}	--	Mater. Chem. Front. 2020, 4 (1), 213-221.
MNSs@NGA	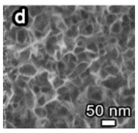	821.3	-0.2-1	1.0 M Na_2SO_4	690.2 at 1 A g^{-1}	563.2 F g^{-1} at 20 A g^{-1}	95.2% after 10 000 cycles at 10 A g^{-1}	This work

CNT/MnO_2/rGO: carbon nanotube@manganese oxide nanosheet core-shell structure encapsulated within reduced graphene oxide film

MnO_2-NHCSs: ultrathin MnO_2 nanoflakes grown on N-doped hollow carbon spheres

Table S2 Comparison of asymmetrical supercapacitor performance between MNSs@NGA and reported MnO_x-based materials

ASC	Morphology	Voltage window / V	Electrolyte	Specific capacitance / F g^{-1}	E / Wh kg^{-1}	P / W kg^{-1}	Cycling stability	Ref.
ACEP@MnO_2//AC	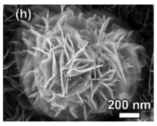	0-2.0	1.0 M Na_2SO_4	111.6 at 0.5 A g^{-1}	31	500	~100% after 5000 cycles at 5 A g^{-1}	ACS Sustainable Chem. Eng. 2018, 6 (1), 633.
MnO_2/GO//HPC		0-2.0	1.0 M Na_2SO_4	52 at 1.0 A g^{-1}	46.7	100	93% after 4000 cycles at 1 A g^{-1}	Small 2015, 11 (11), 1310-1319.
PPy/MnO_2//N-doped mesoporous carbon	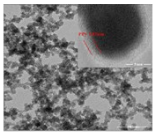	0-2.0	1.0 M Na_2SO_4	69.5 at 0.5 A g^{-1}	38.6	900	90.6% after 5000 cycles at 5 A g^{-1}	Chem. Eng. J. 2017, 307, 105.
yolk–shell MnO_2@MnO_2//AC	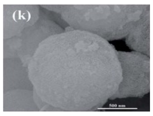	0-1.8	1.0 M Na_2SO_4	90.8 at 1.0 A g^{-1}	40.2	891.2	82% after 10000 cycles at 10 A g^{-1}	J. Mater. Chem. A 2018, 6 (4), 1601.
MnO_2 nanoflakes shell@PPy core//AC	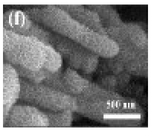	0-2.0	1.0 M Na_2SO_4	57 at 1.0 A g^{-1}	25.8	901.7	90.3% after 6000 cycles at 3 A g^{-1}	Nano Energy 2017, 35, 242.
Mn_3O_4–rGO-2//AC	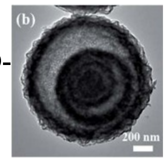	0-1.7	2.0 M KOH	180.2 at 1.0 A g^{-1}	72.3	864.0	93.4% after 5000 cycles at 10 A g-1	J. Mater. Chem. A 2019, 7, 6686-6694.
MNSs@NGA//AC		0-2.0	1.0 M Na_2SO_4	199.0 at 1.0 A g^{-1}	110.6	1000.4	96.2% after 10000 cycles at 5 A g^{-1}	This work

MnO_2/GO//HPC: MnO_2/GO//3D hierarchical porous structure carbon material derived from Artemia cyst shell

Mn_3O_4–rGO-2: Mn_3O_4 hollow spheres with controlled shell numbers in reduced graphene oxide

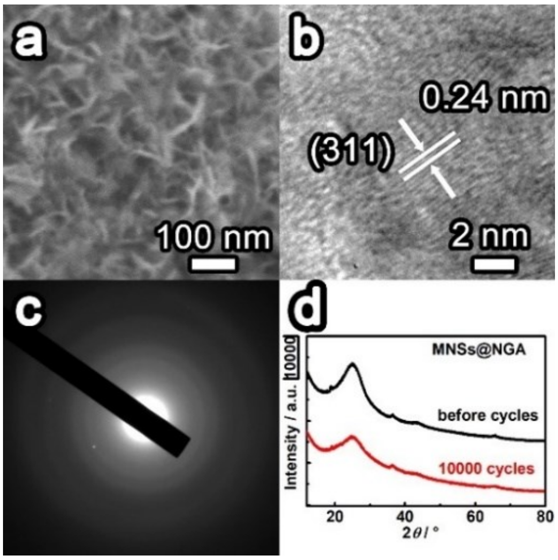

Fig. S6 (a) SEM image, (b) HRTEM image and (c) SAED pattern of MNSs@NGA after cycling stability test. (d) XRD patterns of MNSs@NGA before and after cycling stability test.

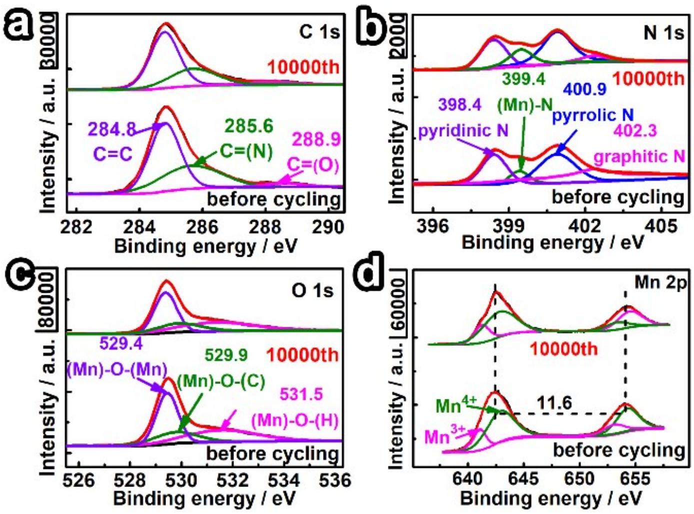

Fig. S7 (a) C 1s, (b) N 1s, (c) O 1s and (d) Mn 2p XPS spectra of MNSs@NGA before and after cycling stability test.

\

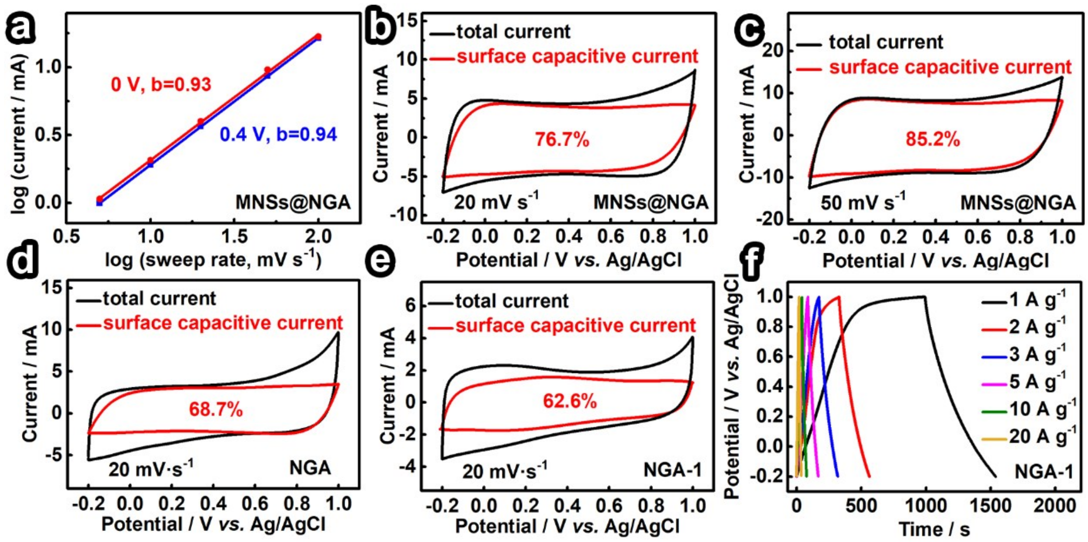

Fig. S8 (a) a plot of log (i) *vs.* log (v) from 5 to 100 mV s^{-1} for MNSs@NGA. Proportion of surface capacitive current contributions of total current of (a) MNSs@NGA at scan rates of (b) 20 and (c) 50 mV s^{-1}. Proportion of surface capacitive current contributions of total current of (d) NGA and (e) NGA-1 at the scan rate of 20 mV s^{-1}. (f) GCD curves at different current densities of NGA-1.

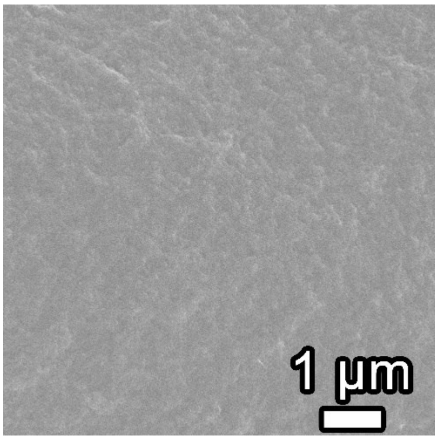

Fig. S9 SEM image of NGA-1.

Table S3 ORR catalytic properties comparison of MNSs@NGA to reported MnO_x-based catalysts

Sample	Morphology	Specific surface area / $m^2\ g^{-1}$	E_{onset} / V	$E_{1/2}$ / V	Tafel slope / mV dec^{-1}	n	Cycling stability	Ref.
Ni-MnO/rGO aerogels	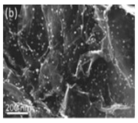	109	0.94	0.78	85	4	93.7% after 10000 s	Adv Mater. 2018, 30, 1704609.
Mn_3O_4/rGO	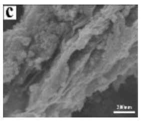	89	0.86	0.76	--	3.96	88.5% after 20000 s	J. Colloid Interface Sci. 2017, 488, 251.
MnO_2/rGO	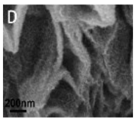	183	0.83	0.69	--	3.85	--	Int. J. Hydrogen Energy 2016, 41, 5260.
Co/MnO	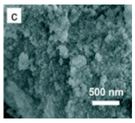	--	0.906	0.819	98	3.89	84.2% after 35000 s	Catal. Sci. Technol. 2018, 8, 480.
MNSs@NGA	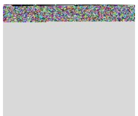	821.3	0.97	0.82	76	3.99	87.2% after 50000 s	This work

GMNCs: Graphene sheets@MnO@ N-doped carbon composites

Co-MONSs/MC: Co ions-doped MnO_2 nanosheets/macroporous carbon composites

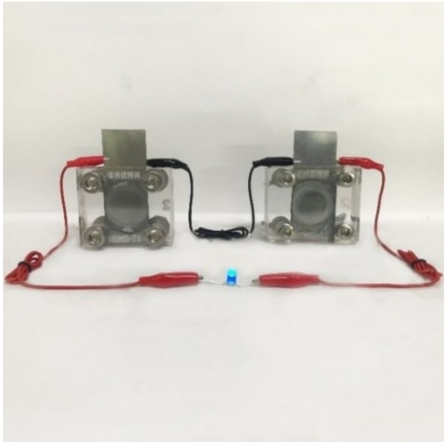

Fig. S10 Photograph of a blue LED (≈ 3 V) lit by two series Zn-air batteries with MNSs@NGA as air cathode after 24 h.

Table S4 Comparison of the performances of Zn-air batteries with reported electrocatalysts

Sample	Electrolyte	Loading mass of catalyst / mg cm^{-2}	Open-circuit voltage / V	P/ mW cm^{-2}	Specific capacity / mAh g_{Zn}^{-1}	E / Wh kg_{Zn}^{-1}	Ref.
FeCo@MNC	6.0 M KOH + 0.20 M $Zn(Ac)_2$	3.2	1.41	115.0	--	--	Appl. Catal. B 2019, 244, 150-158
FeNi@N-GR	6.0 M KOH + 0.20 M $Zn(Ac)_2$	2.0	1.35	85	765	940	Adv. Funct. Mater. 2018, 28 (14), 1706928
Ni_3Fe/N-C sheets	6.0 M KOH + 0.20 M $ZnCl_2$	--	--	--	528	634	Adv. Energy Mater. 2017, 7, 1601172
S-LCO	6.0 M KOH + 0.20 M $Zn(Ac)_2$	2.0	1.47	92	747	--	Chem. Mater. 2020, 32, 3439-3446
$ZnCo_2O_4$/N-CNT	6.0 M KOH + 0.20 M $ZnCl_2$	2.0	1.47	82.3	428.5	595.6	Adv. Mater. 2016, 28, 3777-3784
Co_3O_4 nanoplates	6.0 M KOH + 0.20 M $Zn(Ac)_2$	2.0	--	59.7	702.4	901.6	Energy 2019, 166, 1241-1248
MNSs@NGA	6.0 M KOH + 0.20 M $ZnCl_2$	2.0	1.52	115.0	794.6	961.5	This work

FeCo@MNC: mesoporous Fe/Co-N-C nanofibers with embedding FeCo nanoparticles

FeNi@N-GR: FeNi@N-graphene core-shell nanostructures

Ni_3Fe/N-C: Ni_3Fe nanoparticles embedded in porous nitrogen-doped carbon sheets

S-LCO: S-doped $LaCoO_3$

$ZnCo_2O_4$/N-CNT: $ZnCo_2O_4$/N-doped-CNT

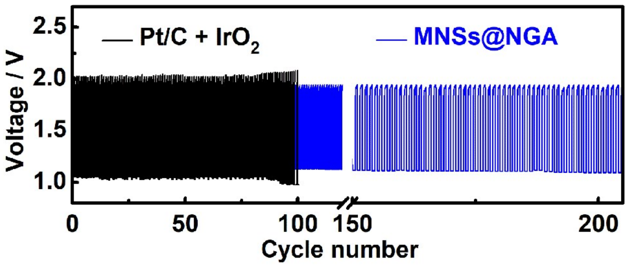

Fig. S11 Long term cycling performance at a constant current density of 10 mA cm^{-2} of Zn-air batteries separately with MNSs@NGA and Pt/C + IrO_2 as air cathode.

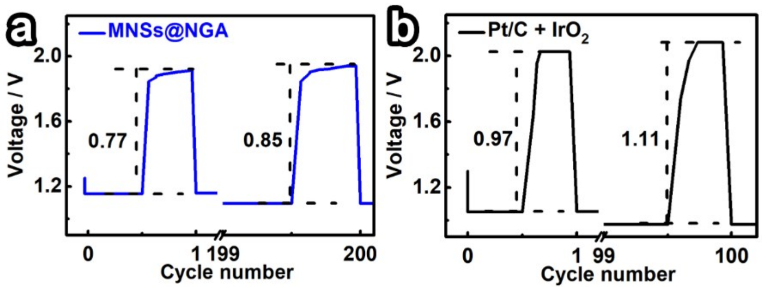

Fig. S12 Enlarged 1st and corresponding cycle (200th and 100th) of the discharge-charge voltage profiles of Zn-air batteries with (a) MNSs@NGA and (b) Pt/C + IrO_2 catalyst as air cathode.

References and notes

1. D. C. Marcano, D. V. Kosynkin, J. M. Berlin, A. Sinitskii, Z. Sun, A. Slesarev, L. B. Alemany, W. Lu and J. M. Tour, *ACS Nano*, 2010, **4**, 4806-4814.

2. J. Xin, R. J. Zhang and W. G. Hou, *J. Mater. Chem. B*, 2014, **2**, 3697-3704.